

The Solution Precursor Plasma Spray Processing of Nanomaterials

E. Brinley, K.S. Babu, and S. Seal

Solution precursor plasma spray (SPPS) synthesis is a simple, single-step, and rapid technique for synthesizing nano-ceramic materials from solution precursors. This innovative method uses molecularly mixed precursors as liquids, avoiding a separate processing method for the preparation of powders and enabling the synthesis of a wide range of metal oxide powders and coatings. Also, this technique is considered to be promising for the formation of non-equilibrium phases in multi-component oxide systems. This short review provides an insight into the important aspects of SPPS, the properties obtained in comparison to conventional plasma spray, and the potential applications of the SPPS process.

INTRODUCTION

The physical and mechanical properties of materials exhibit remarkable improvements as their grain size is reduced from the micrometer to the nanometer range. Various techniques such as sol-gel, vapor deposition, laser ablation, mechanical milling, flame pyrolysis, and radio frequency (RF)- and microwave plasma synthesis have been developed and/or modified to synthesize nanomaterials. A critical look at the status of nanotechnology shows that most of the work has been concentrated on the synthesis of various nanomaterials, but little work has been reported on consolidation of these nanoparticles. Studies carried out to consolidate nanomaterials have shown that these powders have inherent metastability and a strong tendency for rapid grain growth, and that the conventional powder metallurgy techniques such as sintering and hot pressing can lead to difficulties in achieving full consolidation while preserving the nanometer size of the starting materials. Coating

technology that combines the synthesis and consolidation processes into a single operation can be advantageously used to avoid some of the problems encountered during conventional consolidation procedures. Further, many engineering applications such as wear resistance and thermal barrier coatings (TBCs) require enhanced properties at the surface only, indicating that directly depositing as nanomaterials can offer more surface engineering applications than freeform structures.

ROLE OF PLASMA IN PROCESSING MATERIALS

The plasma spray process is a widely used technique for producing surface coatings for various industrial applications.¹ This process uses a high-temperature, high-velocity plasma jet to melt and spray 10–100 μm sized feedstock to form an overlay coating. In general, the plasma spray process uses a solid feedstock and produces fine-grained (0.5 to 5.0 μm) deposits. The feedstock is commonly in the form of powders that need to be prepared separately. Generally, plasma spray processing is used for producing protective and performance-enhancing coatings. The plasma flame has many special characteristics, such as a high enthalpy density, high temperature, high velocity, active environment, and extremely high heating and cooling rates. In plasma spray, these process variables are tuned along with the powder properties to achieve the desired coating characteristics.

SOLUTIONS AS PRECURSORS IN PLASMA SPRAY

Spraying nanopowders in conventional air plasma spray (APS) is problematic, as nanoparticles have low

mass. As a result, they do not possess the required inertia to cross the streamlines of the plasma spray and may lead to segregation on its periphery without depositing on the substrate. Nanosize powders cannot be plasma sprayed owing to their tendency to clog the plasma gun nozzle. High surface friction among fine powder particles leads to inconsistent flow, producing non-homogeneous and inferior coatings. An alternative to the use of dry powders as feedstock is to use solutions in a process known as precursor plasma spray. Solutions can be either in the form of sols (powders dispersed in solvent) or homogeneously dissolved precursor solutions. The former is known as suspension plasma spray (SPS) while the latter is known as solution precursor plasma spray (SPPS).

The precursor solution used in SPPS comprises a metal precursor in the form of nitrates, sulfates, chlorides, or alkoxides dissolved in a suitable medium such as water. Upon injecting the precursor into the plasma flame, the products formed are directed toward the substrate by the carrier gas. Thus, SPPS enables the formation of metal oxides, multi-component composites coupling the process of material preparation and coating into a single step. In the case of SPPS, the precursor is a solution that can enable the formation of nanoparticles as coatings or powders. Since the report of preparation of alumina, zirconia, and yttria-stabilized zirconia nanoparticles and deposits in 1997,² SPPS has been used to process many of the simple as well as complex oxides delivering a wide range of applications including thermal barrier coatings, fuel cells,³ and phosphor,⁴ magnetic,⁵ and biomedical coatings.^{6–8} Solution precursor plasma spray is a versatile process in forming films and coatings for diverse applica-

tions with varying physical properties, as summarized in Table I.

MECHANISTIC ASPECTS OF SPPS

In the plasma synthesis process, first the liquid precursor is atomized and injected into the high-temperature plasma flame. At high temperatures, the material undergoes a reaction to form particles that are collected either as a deposit on a substrate or as a powder. An electrostatic precipitator can also be used to obtain the material in the form of powders. When the atomized droplet enters through the high-temperature flame and is accelerated toward the substrate by the carrier gas, various phenomena can occur affecting the coating properties as shown in Figure 1.

In the SPPS process, a coating forms as a result of multiple sequential steps involving a series of physical and chemical reactions of precursor droplets. The multiple steps consist of the following: precursor droplets form via a liquid atomizer; atomized droplets are rapidly transferred into the plasma region having high temperature and velocity; on entering the plasma region due to the interaction with plasma, the droplets break into a number of tiny droplets; as a result of the smaller size, the solvent evaporates instantly in the hot plasma; the remaining solute undergoes thermal decomposition to form the corresponding

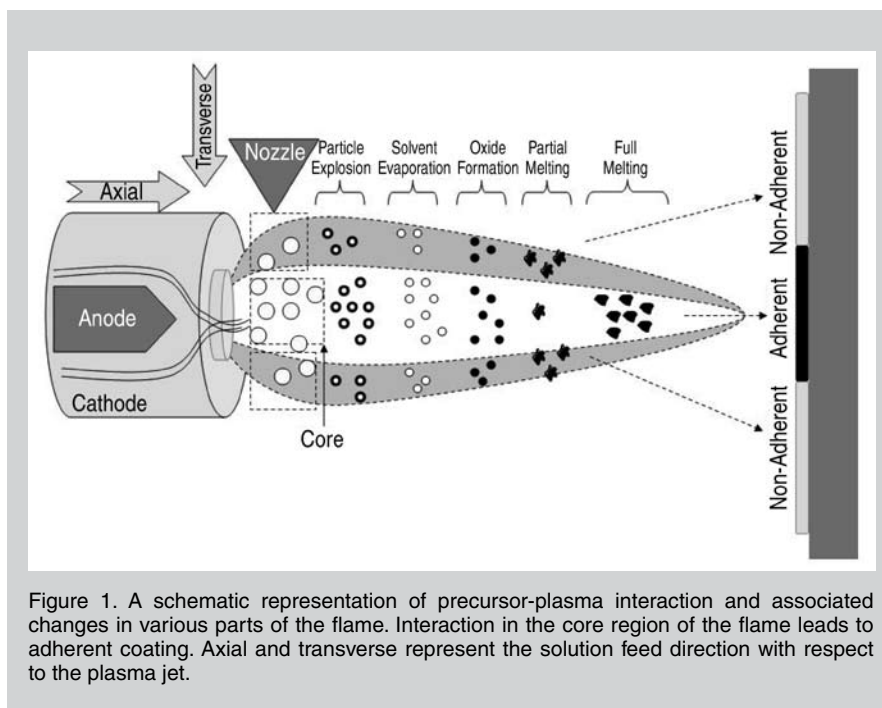


Figure 1. A schematic representation of precursor-plasma interaction and associated changes in various parts of the flame. Interaction in the core region of the flame leads to adherent coating. Axial and transverse represent the solution feed direction with respect to the plasma jet.

oxide particles; they are either partially or fully melted, depending on the residence time of the particle; splat formation on impacting the substrate formation; and the process continues, leading to a dense coating. Depending on the mechanism of interactions between these particles, the formation of large particles, crystals, agglomerates, or aggregates can result. If the droplet spends insufficient time within the plasma flame, incomplete evaporation of the solvent and condensation of the precursor materials occur.

As a result, liquid droplets splash on the substrate surface and then undergo further reactions, depending on time and the availability of thermal energy, leading to the formation of a patchy deposit.

The microstructure of an SPPS coating will be determined by the critical parameters including original droplet momentum, plasma and heat transfer, flight trajectory and residence time of droplets in plasma, and substrate temperature as well. This feature is illustrated in the scanning electron micrograph (SEM) for cerium oxide nanoparticles coated on mild steel substrate exhibiting the surface morphology of fully as well as partially melted particles along with the micron-sized agglomerates (Figure 2). Further, splats with a typical size of less than 1 μm are produced in the SPPS process and a thickness of less than 10 μm can be achieved by controlling the chemical concentration in the solution precursors and solution flow rate. Although the SEM micrograph shows the presence of micron-sized agglomerates, these agglomerates were made up of particles in the nano regime as shown by the high-resolution transmission electron micrograph (HRTEM) images (Figure 2, top inset). The presence of lattice fringes indicates the highly crystalline nature of resultant cerium oxide nanoparticles formed through the SPPS process.

Plasma spray synthesis is a single-step process and all the reactions are

Table I. Various Materials Synthesized by SPPS and Their Potential Applications*

Material System	Coating Thickness (μm)	Particle/Grain Size (nm)	Porosity Vol. (%)	Potential Applications	References
Al_2O_3	—	10–50	—	Nanopowders	2
ZrO_2	—	20–80	—	Nanopowders	2
YSZ	—	20–100	—	Nanopowders	2
CeO_2	1	30–50	—	High-temperature oxidation resistance	9,10
$\text{ZrO}_2\text{-}7\text{Y}_2\text{O}_3$	250–2,000	—	16–30	TBC	11–18
Ni-LDC	100–150	—	40–45	Fuel cell	3
LDC	5	—	—	Fuel cell	3
Eu^{3+} Doped TiO_2	—	30–83	—	Optoelectronics	8
Eu^{3+} Doped Y_2O_3	20–100	500–5,000	—	Luminescent coatings	4
Yttrium Iron Garnet	—	90–110	—	Magneto-optic	4
Hydroxyapatite	3–5	10–25	—	Biomedical	7,8
$\text{ZrO}_2\text{-Al}_2\text{O}_3$	—	10–1,000	—	Metastable	19
$\text{ZrO}_2\text{-Y}_2\text{O}_3\text{-Al}_2\text{O}_3$	—	4–3,000	—	Metastable ceramics	20

*TBC = thermal barrier coatings; LDC = lanthanum doped ceria

driven to completion during the spray processing itself, resulting in the formation of nanosized ceramic particles. No post-spray calcinations or heat treatment is required. Spray synthesis of nanomaterials with consistent characteristics requires control of the size and size distribution of atomized liquid droplets and optimization of spray parameters. As a result, the diameter of the atomic nozzle, the pressure and flow rate of the atomizing gas, and the concentration and flow rate of the liquid feedstock and droplet size distribution must be monitored for optimum coating properties. The heat flux of the plasma flame is governed by the nature of the gases. Generally argon and nitrogen are used as the primary gases while hydrogen is commonly used as a secondary gas. The size, shape, and phase composition of the resulting nanomaterials depend strongly on the spray feedstock.

The SPPS method for the deposition of ceramic coatings offers several advantages over the conventional plasma-spray method, such as circumvention of the powder-feedstock preparation step, better control over the chemistry of the deposit, the ability to deposit compositionally graded coatings with

ease, the ability to deposit coatings that are inherently nanostructured (nanometer-scale grain sizes) and porous, and processing versatility. These advantages and the potential to deposit a wide range of ceramics for the applications of thermal barrier coatings (TBCs), hard coatings, catalyst supports, biomedical implants, and fuel cell components make the SPPS method technologically very attractive. Through the SPPS process, nanostructured ceramic and ceramic-ceramic composite films and coatings and metal-ceramic composites are being developed, mainly for applications in gas turbine engines and solid oxide fuel cells. Different features of SPPS make the process adoptable for a wide variety of applications.

Thermal Barrier Coatings

Thermal barrier coatings are used in applications requiring high temperatures in order to shield the component from the heat, which allows the system to run at a higher temperature, and thus more efficiently.²¹ Applications for this technology focus on turbines, which experience high mechanical stresses and environmental factors resulting from the high heat where reduction of heat would

extend component life.²² Typically, the main load-bearing component is a metal superalloy which is coated with an intermetallic bond coat. The TBC is applied directly to the bond coat; however, during thermal cycling a thermally grown oxide (TGO) grows between them.²² The TBC lowers the temperature of the load-bearing component if the TBC is thick and durable enough to handle the temperature condition at the surface and reduce the gradient created from the surface to the layers beneath.¹ If it is sufficient, the TBC can protect the superalloy from creep or fatigue, thus extending the component's useful life.²³

Two typical processes for application of TBCs are electron-beam physical vapor deposition (EB-PVD) and air plasma spray (APS).²⁴ Thermal barrier coatings applied by EB-PVD are generally stronger than APS-based TBCs due to their lateral strain tolerance that is derived from their columnar structure.²⁵ These columns are arranged perpendicular to the surface, but with this enhancement in strength comes an increase in thermal conductivity. In contrast, APS has a lamellar structure characteristic of the splat formation which lowers thermal conductivity.²⁶ These flat plates hinder heat transfer perpendicular to the coating surface, as do the micro- and macro-cracks created during spraying.²⁵ Unfortunately, although this process is less expensive and has better thermal resistivity, it lacks the structural integrity of EB-PVD TBC coatings. In order to create the best material for TBC applications the advantages of both processes would be combined, giving both high strain tolerance and low thermal conductivity. The low thermal conductivity of SPPS coatings can be understood as vacant dielectric material in the form of pores or cracks. The following equation describes theoretical porosity based upon spherical porosity:²⁷

$$\int \frac{k_{\text{Spherical_pore}}}{k_{\text{Dense}}} = 1 - \frac{3}{2} \phi_{\text{Sphere}}$$

Using SPPS, it is possible to create a high-strength TBC coating due to some unique features that can be created using this process. The first feature is the presence of extremely small splat formation in the SPPS coatings ranging from 1 μm to 10 μm as compared to the typical APS

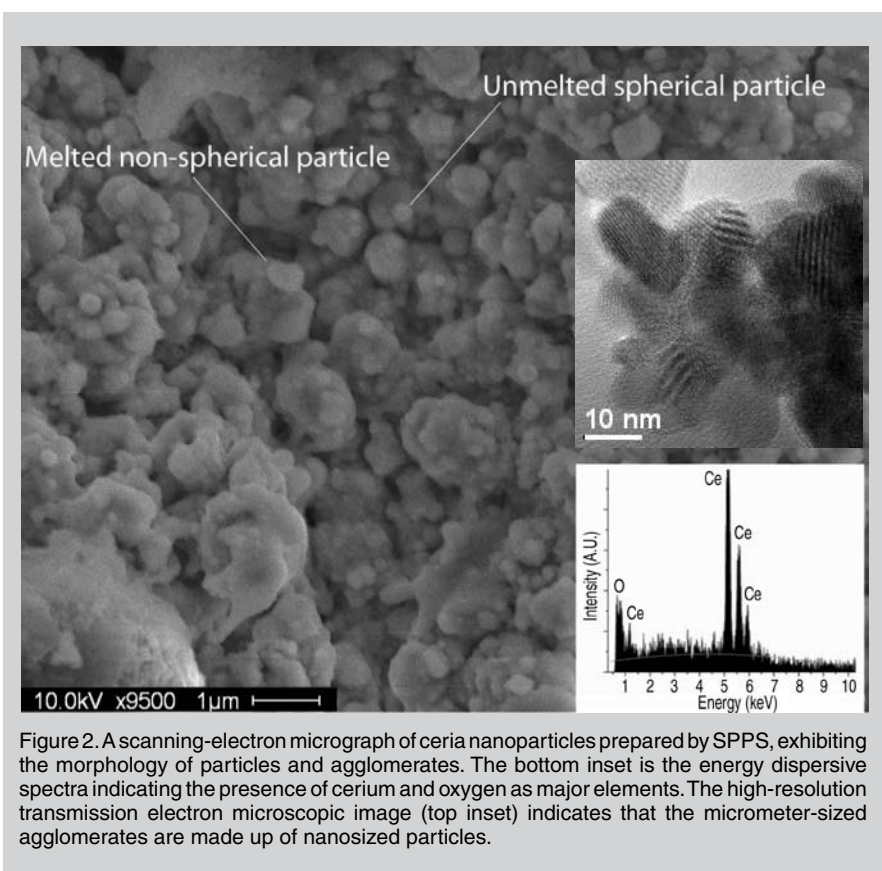


Figure 2. A scanning-electron micrograph of ceria nanoparticles prepared by SPPS, exhibiting the morphology of particles and agglomerates. The bottom inset is the energy dispersive spectra indicating the presence of cerium and oxygen as major elements. The high-resolution transmission electron microscopic image (top inset) indicates that the micrometer-sized agglomerates are made up of nanosized particles.

of 50–100 μm .^{28,29} This finer structure is further enhanced by the columnar and equiaxed grain structures within these splats.^{24,30} The strain tolerance is enhanced further by a unique vertical crack formation that is normal to the coating surface.^{11,27} These vertical cracks manifest themselves as a “mudflat” design when viewed normal to the surface.¹¹ Whereas in thinner coatings the cracks are not connected and appear as disconnected lines in the coating, as coatings become thicker and more stable, large columns interconnect at the surface giving the aforementioned appearance. These through-thickness cracks are not reduced after thermal cycling and remain throughout the lifetime of the coating.³⁰ Thermal barrier coatings formed by SPPS are associated with vertical cracks and fewer horizontal cracks, the characteristic feature of APS. Coating thickness and microstructure, and especially porosity of the coatings, governs the distance between the adjacent vertical cracks and the penetration depth of the cracks. Thus, combining the features of SPPS including small splat formation, minimal splat boundaries, vertical cracks, non-pyrolyzed precursor, and equiaxed grain boundaries, the SPPS process creates durable TBCs as compared to the APS process and rivaling the EB-PVD process.^{11,31} Thermal cycling is another important feature of TBCs and the effect it has on the coating can largely change the life of a particular part. In Table II, the thermal cycles to failure by deposition method are shown, with APS being the weakest and SPPS being the strongest. The SPPS coating’s increased strength is based upon a microstructural difference from that of APS. In addition, the thermal conductivity of SPPS is commensurate with APS, in contrast to that of EB-PVD which has a higher thermal conductivity due to its higher density.

High-temperature oxidation resistance is an important property in determining a technology’s structural applications. Many alloys exhibit better high-temperature oxidation resistance due to the formation of a protective oxide layer (such as Al_2O_3 or Cr_2O_3) on the surface. However, SPPS coated cerium oxide nanoparticles on 410 martensitic stainless steels have shown a 50% reduction of oxidation rate compared to that of uncoated material. The SPPS technique

combined with nanoparticle chemistry can lead to the development of efficient and economic high-temperature oxidation resistant coatings.

Porous Anodes in Solid Oxide Fuel Cells

Solid oxide fuel cells (SOFCs) are a highly efficient, pollution-free technique to produce electricity through electrochemical and chemical reactions between hydrogen/hydrocarbon fuels and oxygen. However, some difficulties associated with SOFCs, involving the fabrication of the cell components, materials selection, high operating temperatures, mechanical and electrochemical reliability, and high production cost have to be overcome before this technology becomes commercially viable.^{3,9} The catalytic activity of an anode is one of the important parameters in determining the performance of SOFCs. A porous microstructure with a large surface area can enhance the interaction of incoming fuel.

The SPPS-deposited anode layer is highly porous, with porosity of 40–45 vol.%, and the thickness of the anode layer is 100–150 μm . The layer consists of a number of submicrometer-sized particles that are partially melted and have a near-sphere shape. Porosity analysis indicated that the porosity distribution varies from 20 nm to 0.5 μm with a central value of 150 nm. Unlike the case of disk-like porosity in conventional plasma spray using a powder feedstock, the SPPS process produces near-sphere-shaped pores that are formed by the stack of the small sphere particles. In the anode layer, it is well known that charge transfer reaction site is located at three-phase-boundaries (TPB) of ionic, electronic, and gas phases. By increasing the number of active sites at the TPB, the catalytic property of the anode, and hence, the efficiency of the SOFC can be improved. Therefore, the nanometer and submicrometer porosity in the SPPS-formed LDC+NiO anode layer can be beneficial for increasing fuel gas permeability and anode catalytic property.

Metastable Ceramic Composites

Generally, metastable ceramics are formed by kinetically suppressing equilibrium phases and microstructures using

rapid processing. Also, rapid solidification leads to metastable ceramics, where the short time scales involved suppress long-range diffusion. However, in both processes the resulting materials are in the form of powders requiring consolidation and subsequent sintering for the fabrication of engineering components. During sintering, solid-state phase transformations can take place, resulting in equilibrium microstructures in the sintered parts. These metastable structures can exist as transient phases or extended solid solutions, and can have unusual electrical, optical, magnetic, thermal, and mechanical properties. Liquid-precursor methods are assuming an important role in processing metastable ceramics, where rapid pyrolytic decomposition of liquid chemical precursors is performed by spraying liquid precursor into reactors. The oxide is generated through the steps of solvent evaporation, low-temperature pyrolysis (or decomposition) of the resulting gel or solid residue, and low-temperature crystallization. The low homologous temperatures involved in pyrolysis and crystallization processes (typically $T/T_M < 0.5$) suppress the long-range diffusion, resulting in transient phases in the case of single-component precursors or extended solid solutions in the case of multi-component precursors. Pure ZrO_2 , $\text{ZrO}_2\text{-Al}_2\text{O}_3$ as well as $\text{ZrO}_2\text{-Y}_2\text{O}_3\text{-Al}_2\text{O}_3$ systems were deposited by SPPS.^{20,35} In the binary 10 $\text{Al}_2\text{O}_3\text{-90ZrO}_2$ system, two structural regimes, one with nanostructures (10–40 nm) containing tetragonal zirconia and other of 50–100 nm with primarily monoclinic zirconia, were found. It was shown that Al^{3+} forms a solid solution with ZrO_2 , which is otherwise insoluble at room temperature.

Biomedical Coatings

Hydroxyapatite [HA , $\text{Ca}_{10}(\text{PO}_4)_6(\text{OH})_2$] has been widely used as a coating to improve the fixation of implants to bone. It is known to be an osteoconductive material and can promote bone growth at the surface of the implant. A submicrometer/nanocrystalline HA coating was made from inexpensive liquid precursors.⁷ Using an organic sol-gel solution of calcium nitrate tetrahydrate and triethyl phosphate, porous HA coatings were formed on a Ti-6Al-4V substrate.⁶ The coating exhibited microstructural features typically found in solution

Table II. Thermal Cycles to Failure for EB-PVD, APS, and SPPS Coating Techniques for YSZ

Process	Thermal Cycles to Failure	References
APS	40–400	32–34
EB-PVD	675	33
SPPS	400–1,000	33,34

precursor plasma spray processes; a combination of melted and unmelted deposits and small hollow spheres. Nanocrystalline HA coatings can improve the resorption of the coating in the body, avoiding the irritant effect of larger particles normally obtained from air plasma spray.

Luminescent and Magnetic Materials

Rare earth metal ions such as Eu^{3+} are doped into oxides or semiconductors to improve the phosphorescence properties, but effective doping by wet chemical methods is still difficult as the dopant and host ions differ in ionic sizes as well as chemical properties, leading to variations in precipitation kinetics. As a result, these rare earth ions might be simply absorbed on the surface of the particles and the observed light emission is due to the direct absorption of rare earth ions rather than due to the host matrix effect. Also, very often wet chemical methods lead to amorphous or low crystalline particles requiring thermal treatment to induce crystallinity. The presence of surface functional groups such as hydroxyls can lead to nonradiative relaxations limiting the applications of these materials. Eu^{3+} -doped TiO_2 and Y_2O_3 luminescent nanocrystals,^{4,36} with efficient nonradiative energy transfer from the host to the activator Eu^{3+} ions, were synthesized by the precursor plasma technique.

In the case of a titania matrix, it was found that an increase in Eu^{3+} content leads to an increase in rutile phase fraction. The observed red emissions were intense compared to those of the powders prepared by other methods due to efficient nonradiative energy transfer from the matrix to Eu^{3+} ions, enabling their applications in optoelectronic devices.³⁶ Yttrium iron garnet ($\text{Y}_3\text{Fe}_5\text{O}_{12}$, YIG) is a well-known magnetic material used for applications in telecommunications

and data storage. Conventional methods used higher temperatures for processing and resulted in wider particle size distribution. Also, maintaining the proper stoichiometry was difficult, which directly affects the magnetic properties. Recently, YIG was formed through a single-step precursor plasma process.⁵

Deposition Mechanism and Modeling

Coatings by SPPS have unique properties based upon their structural differences as compared to other thermal spray processes. The basic understanding of the mechanism is a series of steps that occur in order from the time the solution is atomized into the flame to its final impinging on a surface to become a coating. The series begins with solvent evaporation, gelation, pyrolysis, crystallization, sintering, and possibly melting and resolidification.³⁵ Each droplet does not necessarily experience the complete cycle due to the temperature of the flame, either core or periphery, or because the total time in the flame is not sufficient to complete. The flame has two distinct regions: a core ($>2,000^\circ\text{C}$) and a periphery ($<2,000^\circ\text{C}$) where a droplet would not experience the full thermal cycle and could therefore be at a different stage of crystallinity or have different size or morphology. A sub-process of the above thermal series can be understood by solute migration to the outside of a precursor droplet ($\sim 38 \mu\text{m}$), through evaporation of solvent becoming solid ($\sim 8 \mu\text{m}$) and impermeable to gas. As the temperature increases inside the hard shell, the gas ruptures the shell creating the $1 \mu\text{m}$ adherent particles found at the core of a SPPS coating. Stages of this process are shown in the large hollow spheres and powdery deposits that are characteristic of the regions adjacent to the core in coatings.³⁷

Negative effects can be avoided, such as low deposition efficiency, bubble formation, and non-adherence. Deposition efficiency is a product of the aforementioned temperature regions whereby there is a Gaussian profile of coating thickness. This is minimized by altering process parameters to maximize deposition from the core region and minimize that of periphery or rastering the spray. Bubble formation results from segregation of solute toward the

outside, forming a solid shell which resists particle explosion, typical of SPPS, if it becomes too thick.³⁸ This is thought to occur in lower-temperature regions where the rate of vaporization is low and is dependent on the depth of penetration of the precursor droplets in the flame. Along with bubble formation, non-adherence is found at areas beyond the core where droplets experience lower heat gradients and are at various stages of crystallization or melting.²⁸

Modeling of SPPS begins with deciding upon certain basic setup criteria including atomization location transversely or axially to the flame, which would result in less or more particles focused at the center of the flame. Transverse is the model standard. Heat and mass transfer around individual droplets are modeled according to velocity and temperature. The solute amounts and different precipitate areas are numerically modeled and predicted according to averaged values and single, non-interacting particle movement. The droplet properties can be modeled as if inside the plasma medium and are estimated according to instantaneous values of location and size. By varying parameters and understanding both thermodynamic and physical properties of the plasma environment multiple calculated scenarios are generated.³⁹

The limitations of modeling are similar for any modeling process and do not detract from the benefit in so much as the virtual SPPS envisioned by calculated values in only a discrete setting. Real SPPS processing would involve multiple mechanisms simultaneously and continuously interacting. For example, droplet size is chosen as is initial trajectory; however, secondary drag forces are neglected and the calculated injection depth, particle velocity, and subsequent evaporation rates based upon particle position within the flame are deduced from experimentally derived plasma temperature and velocity values. By understanding the phenomena better optimization of process parameters can be achieved reducing extraneous trials to deduce parameters.³⁸

FUTURE TRENDS

The SPPS process has many possibilities for multiple applications that are only partially realized. Thermal

barrier coatings already show a marked increase in thermal cycles to failure as compared to their APS and EB-PVD counterparts and equivalent thermal conductivity values as APS. In addition, the ease of processing by removing the powder formation/agglomeration stage makes SPPS simpler and quicker for TBCs. The porosity control afforded by SPPS processing enables its usage in catalytic applications where reduction of activation energy results in lower operating temperatures. Therefore, the incorporation of solution-based plasma in industrial applications can be expected to increase. The strong control of the stoichiometry of SPPS opens many avenues of exploration including biomaterials, which should see an increased focus due to the need for exact composition control and porosity control. Non-equilibrium processing, such as is needed for luminescent and magnetic materials, can be realized at lower temperatures and with more accuracy for single-step creation of advanced pure and doped ceramics. Modeling by SPPS has been essential to understanding the complicated behavior of particles in the flame. Since this has been explored from the beginning of SPPS research, expect it to be a staple in the future of SPPS.

ACKNOWLEDGEMENT

The authors acknowledge the funding support for plasma nanomanufacturing of novel materials from the Office of Naval Research (ONR) YIP N000140210591, DURIP (ONR N000140310858), Siemens Westinghouse, Pratt and Whitney, and Florida High Tech Corridor.

References

1. P. Fauchais et al., "Developments in Direct Current Plasma Spraying," *Surface & Coatings Technology*, 201 (2006), pp. 1908–1921.
2. J. Karthikeyan et al., "Plasma Spray Synthesis of Nanomaterial Powders and Deposits," *Materials Science and Engineering A*, 238 (1997), pp. 275–286.
3. X. Ma et al., "Solid Oxide Fuel Cell Development by Using Novel Plasma Spray Techniques," *Journal of Fuel Cell Science and Technology*, 2 (2005), pp. 190–196.
4. P.S. Devi et al., "Single-Step Deposition of Eu-Doped Y_2O_3 Phosphor Coatings through a Precursor Plasma Spraying Technique," *Journal of Materials Research*, 17 (2002), pp. 2771–2774.
5. X.Z. Guo et al., "Synthesis of Yttrium Iron Garnet (YIG) by Citrate–Nitrate Gel Combustion and Precursor Plasma Spray Processes," *Journal of Magnetism and Magnetic Materials*, 295 (2005), pp. 145–154.
6. T.W. Coyle et al., "Plasma Spray Deposition of Hydroxyapatite Coatings from Sol Precursors," *Materials Science Forum*, 539-543 (2007), pp. 1128–1133.
7. A. Ioncea et al., "Bioactive Coatings Based on Hydroxyapatite," *Key Engineering Materials*, 132-136 (1997), pp. 1532–1535.
8. E. Garcia et al., "Hydroxyapatite Coatings Produced by Plasma Spraying of Organic Based Solution Precursor," *Ceramic Engineering and Science Proceedings, Advances in Bioceramics and Biocomposites II—A Collection of Papers Presented at the 30th International Conference on Advanced Ceramics and Composites*, 27 (2006), pp. 103–110.
9. F. Gitzhofer, M. Bonneau, and M. Boulos, "Double Doped Ceria Electrolyte Synthesized by Solution Plasma Spraying with Induction Plasma Technology," *Thermal Spray 2001: New Surfaces for a New Millennium*, ed. C.C. Berndt, K.A. Khor, and E.F. Lugscheider (Materials Park, OH: ASM International, 2001), pp. 61–68.
10. V. Viswanathan et al., "High-Temperature Oxidation Behavior of Solution Precursor Plasma Sprayed Nanoceria Coating on Martensitic Steels," *Journal of the American Ceramic Society*, 90 (2007), pp. 870–877.
11. A.D. Jadhav et al., "Thick Ceramic Thermal Barrier Coatings with High Durability Deposited using Solution-Precursor Plasma Spray," *Materials Science and Engineering A*, 405 (2005), pp. 313–320.
12. L. Xie et al., "Deposition of Thermal Barrier Coatings using the Solution Precursor Plasma Spray Process," *Journal of Materials Science*, 39 (2004), pp. 1639–1646.
13. P.P. Nitin et al., "Towards Durable Thermal Barrier Coatings with Novel Microstructures Deposited by Solution Precursor Plasma Spray," *Acta Materialia*, 49 (2001), pp. 2251–2257.
14. L. Xie et al., "Formation of Vertical Cracks in Solution-Precursor Plasma-Sprayed Thermal Barrier Coatings," *Surface & Coatings Technology*, 201 (2006), pp. 1058–1064.
15. X. Ma et al., "Low Thermal Conductivity Thermal Barrier Coating Deposited by the Solution Plasma Spray Process," *Surface & Coatings Technology*, 201 (2006), pp. 4447–4452.
16. A.D. Jadhav et al., "Low-Thermal-Conductivity Plasma-Sprayed Thermal Barrier Coatings with Engineered Microstructures," *Acta Materialia*, 54 (2006), pp. 3343–3349.
17. L. Xie et al., "Phase and Microstructural Stability of Solution Precursor Plasma Sprayed Thermal Barrier Coatings," *Materials Science and Engineering A*, 381 (2004), pp. 189–195.
18. L. Xie et al., "Deposition Mechanisms of Thermal Barrier Coatings in the Solution Precursor Plasma Spray Process," *Surface and Coatings Technology*, 177-178 (2004), pp. 103–107.
19. A.L. Vasiliev, P.P. Nitin, and X. Ma, "Coatings of Metastable Ceramics Deposited by Solution-Precursor Plasma Spray: I. Binary ZrO_2 - Al_2O_3 System," *Acta Materialia*, 54 (2006), pp. 4913–4920.
20. A.L. Vasiliev and N.P. Padture, "Coatings of Metastable Ceramics Deposited by Solution-Precursor Plasma Spray: II. Ternary ZrO_2 - Y_2O_3 - Al_2O_3 System," *Acta Materialia*, 54 (2006), pp. 4921–4928.
21. W.G. Mao et al., "Modeling of Residual Stresses Variation with Thermal Cycling in Thermal Barrier Coatings," *Mechanics of Materials*, 38 (2006), pp. 1118–1127.
22. A.G. Evans, M.Y. He, and J.W. Hutchinson, "Mechanics-Based Scaling Laws for the Durability of Thermal Barrier Coatings," *Progress in Materials Science*, 46 (2001), pp. 249–271.
23. A.G. Evans et al., "Mechanisms Controlling the Durability of Thermal Barrier Coatings," *Progress in Materials Science*, 46 (2001), pp. 505–553.
24. X. Liangde et al., "Deposition of Thermal Barrier Coatings using the Solution Precursor Plasma Spray Process," *Journal of Materials Science*, 39 (2004), pp. 1639–1646.
25. K. Bobzin, E. Lugscheider, and R. Nickel, "Modeling and Simulation in the Production Process Control and Material Property Calculation of Complex Structured EB-PVD TBCs," *Computational Materials Science*, 39 (2007), pp. 600–610.
26. X. Ning et al., "Modification of Microstructure and Electrical Conductivity of Plasma-Sprayed YSZ Deposit through Post-Densification Process," *Materials Science and Engineering: A*, 428 (2006), pp. 98–105.
27. A.D. Jadhav et al., "Low-Thermal-Conductivity Plasma-Sprayed Thermal Barrier Coatings with Engineered Microstructures," *Acta Materialia*, 54 (2006), pp. 3343–3349.
28. L. Xie et al., "Identification of Coating Deposition Mechanisms in the Solution-Precursor Plasma-Spray Process using Model Spray Experiments," *Materials Science and Engineering A*, 362 (2003), pp. 204–212.
29. S. Sampath et al., "Substrate Temperature Effects on Splat Formation, Microstructure Development and Properties of Plasma Sprayed Coatings Part I: Case Study for Partially Stabilized Zirconia," *Materials Science and Engineering A*, 272 (1999), pp. 181–188.
30. L. Xie et al., "Phase and Microstructural Stability of Solution Precursor Plasma Sprayed Thermal Barrier Coatings," *Materials Science and Engineering A*, 381 (2004), pp. 189–195.
31. S. Guo and Y. Kagawa, "Effect of Thermal Exposure on Hardness and Young's Modulus of EB-PVD Yttria-Partially-Stabilized Zirconia Thermal Barrier Coatings," *Ceramics International*, 32 (2006), pp. 263–270.
32. N.P. Padture et al., "Towards Durable Thermal Barrier Coatings with Novel Microstructures Deposited by Solution Precursor Plasma Spray," *Acta Materialia*, 49 (2001), pp. 2251–2257.
33. A. Jadhav et al., "Thick Ceramic Thermal Barrier Coatings with High Durability Deposited Using Solution-Precursor Plasma Spray," *Materials Science and Engineering: A*, 405 (2005), pp. 313–320.
34. M. Gell et al., "Mechanisms of Spallation of Solution Precursor Plasma Spray Thermal Barrier Coatings," *Surface & Coatings Technology*, 188-189 (2004), pp. 101–106.
35. A.L. Vasiliev, N.P. Padture, and X. Ma, "Coatings of Metastable Ceramics Deposited by Solution-Precursor Plasma Spray: I. Binary ZrO_2 - Al_2O_3 System," *Acta Materialia*, 54 (2006), pp. 4913–4920.
36. J. Li et al., "Phase Structure and Luminescence Properties of Eu^{3+} -Doped TiO_2 Nanocrystals Synthesized by Ar/O_2 Radio Frequency Thermal Plasma Oxidation of Liquid Precursor Mists," *Journal of Physical Chemistry B*, 110 (2006), pp. 1121–1127.
37. L. Xie et al., "Deposition Mechanisms of Thermal Barrier Coatings in the Solution Precursor Plasma Spray Process," *Surface and Coatings Technology*, 177-178 (2001), pp. 103–107.
38. A. Ozturk and B.M. Cetegen, "Modeling of Plasma Assisted Formation of Precipitates in Zirconium Containing Liquid Precursor Droplets," *Materials Science and Engineering A*, 384 (2004), pp. 331–351.
39. A. Ozturk and B.M. Cetegen, "Modeling of Axially and Transversely Injected Precursor Droplets into a Plasma Environment," *International Journal of Heat and Mass Transfer*, 48 (2005), pp. 4367–4383.

S. Seal is a professor, K.S. Babu is a research associate, and E. Brinley is a graduate student with the Surface Engineering and Nanotechnology Facility, Advanced Materials Processing and Analysis Center, Mechanical Materials and Aerospace Engineering, Nanoscience and Technology Center, University of Central Florida, Orlando, Florida. S. Seal can be reached at sseal@mail.ucf.edu.